

# Relation of Bulk-to-Shear Loss Factors in Viscoelastic Auxetic Metamaterials

Simon Preston,\* Julián Londoño-Monsalve, and Ken E. Evans

This article explores the dynamic properties of isotropic auxetic viscoelastic materials, emphasizing the relationships between dynamic bulk and shear moduli, dynamic Poisson's ratio, and energy dissipation. By extending established theories to the negative Poisson's ratio range, it is demonstrated that these relationships remain valid and reveal how dynamic Poisson's ratio impacts Poisson to shear and bulk-to-shear loss factor ratios. Building on Pritz's foundational work, it is shown that it accurately predicts the bulk-to-shear loss factor ratio for auxetic materials. The findings identify the bounds of these ratios within the auxetic range, offering new insights into the behavior of auxetic materials compared to conventional viscoelastic solids. These results are significant for applications requiring advanced damping and energy absorption, such as in defense, sports, and vibration control. The ability to tailor dynamic properties of materials for enhanced performance in these fields is crucial.

## 1. Introduction

Auxetic materials<sup>[1]</sup> display a negative Poisson's ratio,<sup>[2]</sup> expanding laterally when stretched and contracting laterally when compressed (Figure 1a,b). As Poisson's ratio is scale-independent, negative values can arise either from atomic properties,<sup>[1,3–5]</sup> microstructures,<sup>[6–13]</sup> or at larger length scales (Figure 1c–e), provided the Poisson's ratio is measured over length scales larger than the geometry causing it.

Mechanisms of auxeticity can be observed across both 2D and 3D structural models that exhibit negative Poisson's ratio, including reentrant or concave honeycombs (Figure 1c), chiral (Figure 1d) and antichiral lattices, rotating rigid units composed of squares (Figure 1e), rectangles, or triangles, along with liquid crystalline polymers, dilating triangles, egg-rack structures, sinusoidal ligaments, metamaterials, and periodic microstructures

(such as square arrays of circular or elliptical holes in an elastomeric matrix), among other systems.<sup>[14,15]</sup> Auxetic materials exhibit unique and enhanced mechanical properties such as synclastic curvature during bending, deformation-dependent permeability, certain hard-body behaviors,<sup>[16–18]</sup> high shear stiffness,<sup>[19]</sup> thermal expansion,<sup>[20–22]</sup> refractive index,<sup>[23]</sup> exceptional indentation resistance, enhanced fracture resistance capabilities, negative compressibility,<sup>[24–27]</sup> improved fracture toughness and permittivity,<sup>[28]</sup> alongside high sound absorption,<sup>[29,30]</sup> superior damping,<sup>[31]</sup> and energy absorption.<sup>[32,33]</sup>

Although the concept of materials with a negative Poisson's ratio has existed for a century,<sup>[34]</sup> simple mechanical<sup>[35–37]</sup> and thermodynamical<sup>[3,38]</sup> models show auxetic

behavior was realized in the 1980s. Research into auxetics grew rapidly after the nascent works of Evans<sup>[1]</sup> (who coined the word “auxetic” from the ancient Greek “auxetos”) and Lakes<sup>[10]</sup> brought them to the forefront of modern engineering in the early 1990s. Research on auxetic metamaterials spans multiple fields, including acoustics,<sup>[39,40]</sup> seismology,<sup>[41,42]</sup> classical mechanics,<sup>[43–45]</sup> and damping.<sup>[46,47]</sup> They are increasingly researched and integrated into engineering applications, offering innovative solutions in areas such as vibration damping response of auxetic structures (auxetic and nonauxetic structures show different static and dynamic properties),<sup>[29,30,48–50]</sup> blast resistance of sandwich panels with auxetic core,<sup>[30,48,49,51]</sup> compressive behavior of the auxetic cellular structure,<sup>[52,53]</sup> acoustic,<sup>[40,54]</sup> defense,<sup>[32]</sup> sports equipment,<sup>[55]</sup> medical devices,<sup>[56]</sup> clothing,<sup>[33]</sup> packing materials and shock absorption,<sup>[57]</sup> and piezoelectric devices.<sup>[58–61]</sup>

Despite significant advancements in modeling<sup>[62]</sup> and experimental studies of auxetic metamaterials,<sup>[63]</sup> understanding their damping characteristics loss factors is in its early stages.<sup>[64]</sup> Studies show that auxetic materials exhibit enhanced vibration damping capabilities compared to conventional materials. Research on auxetic honeycomb sandwich panels with polyurethane metal laminate face sheets revealed that including an auxetic layer significantly increased the damping loss factor.<sup>[65]</sup> This includes viscoelastic layers within the honeycomb cell walls, where the overall damping performance of the structure improved.<sup>[66]</sup> Analyses of auxetic beams have also shown superior vibration isolation behavior and frequency response over a wide range of frequencies compared to traditional beam structures.<sup>[67]</sup>

Finite element analysis has been used in studies with high accuracy to experimental results,<sup>[68]</sup> including to show a

S. Preston, J. Londoño-Monsalve, K. E. Evans  
Faculty of Environment, Science and Economy,  
Department of Engineering  
University of Exeter  
Stocker Road, Exeter EX4 4PY, UK  
E-mail: sp985@exeter.ac.uk

 The ORCID identification number(s) for the author(s) of this article can be found under <https://doi.org/10.1002/pssb.202400512>.

© 2025 The Author(s). physica status solidi (b) basic solid state physics published by Wiley-VCH GmbH. This is an open access article under the terms of the Creative Commons Attribution License, which permits use, distribution and reproduction in any medium, provided the original work is properly cited.

DOI: 10.1002/pssb.202400512

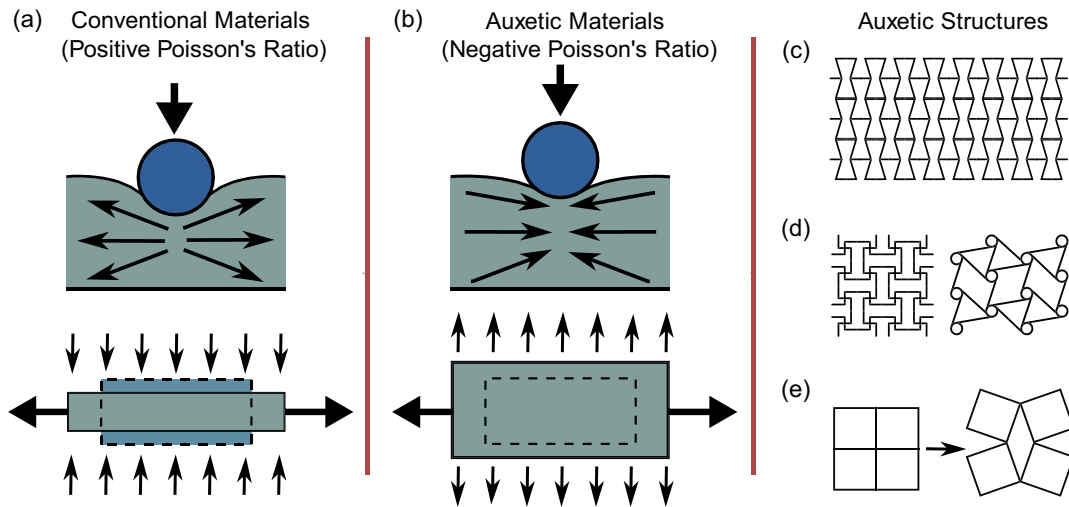


**Figure 1.** a) Conventional (adapted from ref. [6]) and b) auxetic material behavior (adapted from ref. [6]); auxetic structure type: c) bowtie, d) chiral, and e) rotating squares/origami.

significant influence of Poisson's ratio on contact pressure and indentation for the impact behavior of structures,<sup>[69]</sup> especially for extremely negative values close to  $-1$ . Finite element analysis can also be used to obtain structures with nonintuitive characteristics through material topology optimization.<sup>[70]</sup>

The dynamic bulk modulus,  $K_d$ , and shear modulus,  $G_d$ , of a viscoelastic solid can both be expressed in terms of its dynamic elastic (Young's) modulus,  $E_d$ , and dynamic Poisson's ratio,  $\nu_d$ ,<sup>[71,72]</sup>

$$K_d = \frac{E_d}{3(1 - 2\nu_d)} \quad (1)$$

$$G_d = \frac{E_d}{2(1 + \nu_d)} \quad (2)$$

As Poisson's ratio approaches 0.5, as observed in rubbery solids, the dynamic bulk modulus significantly exceeds the

dynamic shear modulus, rendering the material effectively incompressible (**Figure 2a**). As  $\nu_d$  approaches  $-1.0$ , the material becomes highly compressible yet resistant to shear, maintaining structural integrity under load. While the relationship between mechanical properties and Poisson's ratio is well documented for materials with positive Poisson's ratios, there is comparatively less exploration and understanding of this relationship in the context of auxetic viscoelastic materials.<sup>[73-77]</sup>

Using the standard notion for complex shear and bulk moduli, and complex Poisson's ratio,

$$\bar{K}(i\omega) = K_d(\omega)(1 + i\eta_K(\omega)) \quad (3)$$

$$\bar{G}(i\omega) = G_d(\omega)(1 + i\eta_G(\omega)) \quad (4)$$

$$\bar{\nu}(i\omega) = \nu_d(\omega)(1 + i\eta_\nu(\omega)) \quad (5)$$

where  $\bar{K}$  is the complex bulk modulus,  $\bar{G}$  is the complex shear modulus,  $\bar{\nu}$  is the complex Poisson's ratio,  $\nu_d$  is the dynamic

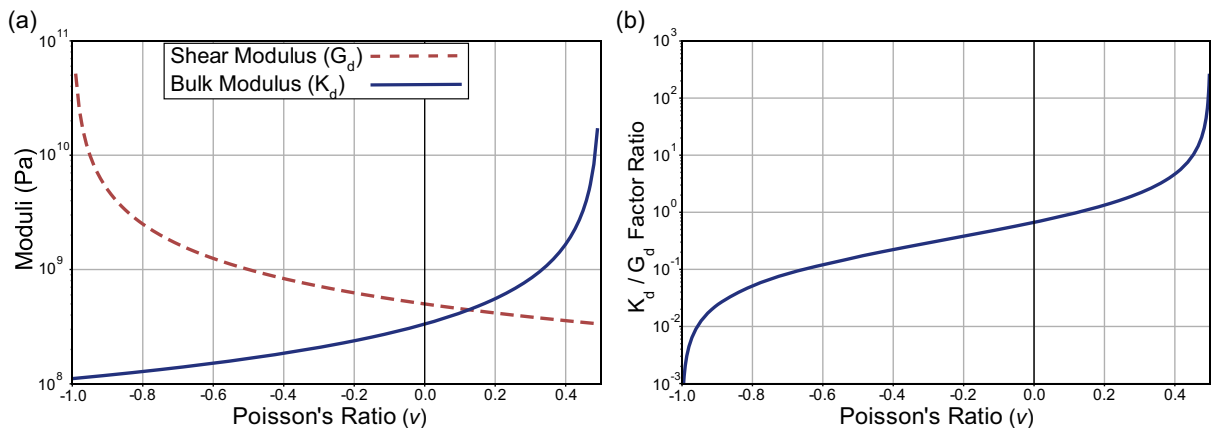


**Figure 2.** a) Dynamic bulk and shear storage moduli (log) change over dynamic Poisson's ratio range  $-1.0 < \nu < 0.5$  (for high-density polyethylene (HDPE)) from Equation (1) and (2) and b) bulk/shear ( $K_d/G_d$ ) storage ratio (log) variation with dynamic Poisson's ratio ( $-1.0 < \nu_d < 0.5$ ) for HDPE using Equation (6).

Poisson's ratio,  $i = \sqrt{-1}$ ,  $\omega = 2\pi f$  (where  $f$  is the frequency in Hz), and  $\eta_K$ ,  $\eta_G$ , and  $\eta_\nu$  are the loss factors for bulk, shear, and Poisson's ratio, respectively.

The concept of Poisson's ratio is typically defined for static or quasistatic loading and represents the ratio of lateral strain-to-axial strain in response to an applied stress. The dynamic Poisson's ratio ( $\nu_d$ ) extends this concept to dynamic or oscillatory conditions, capturing frequency-dependent behavior (Equation 3–5) due to viscoelastic effects, internal damping, and inertia. These deformation mechanisms significantly affect dynamic moduli and energy dissipation. While the static Poisson's ratio is a scalar and constant for a linear elastic material, the dynamic Poisson's ratio is often expressed as a complex quantity (Equation 5).

The bulk and shear loss factors ( $\eta_K$  and  $\eta_G$ ) reflect energy dissipation (including attenuation of bulk and shear wave propagation) through deformation and quantify the amount of energy dissipated per cycle of volumetric or shear deformation due to internal friction. Generally,  $\eta_K$  or  $\eta_G \approx 0$  indicates that the material exhibits very low bulk or shear damping and behaves elastically, with negligible energy dissipation. When  $\eta_K$  or  $\eta_G \rightarrow 1$ , it suggests significant energy dissipation, where the imaginary part of the complex modulus is comparable to its real part, which reflects the material's capacity to store energy. A higher loss factor,  $\eta_K$  or  $\eta_G > 1$ , implies very high energy dissipation during deformation, often as heat or internal friction. The loss factors  $\eta_K$ ,  $\eta_G$ , and  $\eta_\nu$  are influenced by several mechanical and geometrical parameters, including material composition, frequency of loading, temperature, microstructure, density and porosity, geometry and dimensions, and prestrain or recompression. By considering these parameters, the relationship between the loss factors and the physical behavior of the material under dynamic loading can be better understood and tailored for specific applications.

Notice that the dynamic bulk-to-shear storage ratio can be derived from Equation (1) and (2) as a function of the material dynamic Poisson's ratio only<sup>[78]</sup> to get

$$\frac{K_d}{G_d} = \frac{2(1 + \nu_d)}{3(1 - 2\nu_d)} \quad (6)$$

This expression highlights how dynamic Poisson's ratio affects the material's ability to store energy in volumetric versus shear deformation. Equation (6) also shows how this storage ratio is dominated by bulk dynamic storage at  $\nu_d = 0.5$  and shear dynamic storage at  $\nu_d = -1.0$  (see Figure 2b).

The bulk-to-shear loss factor ratio ( $\eta_K/\eta_G$ ) of solid viscoelastic materials is an insightful measure of how energy is dissipated within the material under mechanical stress. Section 2 will elaborate on defining this ratio. From a physical meaning, a ratio of  $0 < \eta_K/\eta_G < 1$  indicates that the material dissipates more energy in shear deformation compared to bulk deformation. This is typical for viscoelastic materials with a positive Poisson's ratio. A ratio of  $\eta_K/\eta_G \approx 1$  is rare but can occur under specific conditions or in specially engineered materials. Conversely,  $\eta_K/\eta_G > 1$  indicates materials where volumetric effects, such as compression or expansion, dominate over shear deformations. This can occur in isotropic loading in soft materials (foams), cyclic compression, and hydrostatic loading conditions where bulk deformation

mechanisms, rather than shear, are the primary contributors to the overall viscoelastic response.

Experiments since the 1960s<sup>[79–81]</sup> have demonstrated that, while independent of each other, the bulk loss factor is smaller than the shear loss factor in the positive Poisson's ratio range. These experimental observations have informed the development of models for viscoelastic solids, particularly regarding projections between the Poisson's to shear and bulk-to-shear loss factors, which are further elaborated in Section 2.1. It is important to note that previous studies<sup>[32,46,71,82–86]</sup> have primarily focused on viscoelastic solids with positive dynamic Poisson's ratios.

This article investigates Poisson's to shear and bulk-to-shear loss factors as a measure of the energy dissipated in a system relative to the energy stored within it,<sup>[7,9,78,79]</sup> comparing these loss factors over a negative Poisson's ratio range using fundamental equations derived by Tschoegl and Pritz.<sup>[82,85,87]</sup> The investigation will be limited to isotropic viscoelastic auxetic materials.<sup>[88]</sup>

## 2. Experimental Section

### 2.1. Poisson to Shear Loss Factor Ratio

Pritz<sup>[82]</sup> initially investigated the link between Poisson and shear loss factors as a function of dynamic Poisson's ratio. This relationship, where  $n$  is an empirical fit to experimental data, is expressed as<sup>[87]</sup>

$$\frac{\eta_\nu}{\eta_G} = \frac{2}{3} \nu_d^{n-1} (1 + \nu_d)(1 - 2\nu_d) \quad (7)$$

At a dynamic Poisson's ratio of 0.5, the material is incompressible, meaning that during compression, the axial and lateral strains adjust to maintain a constant volume (as  $\bar{K} = \infty$ ). In this case, the Poisson's loss factor ( $\eta_\nu$ ) becomes zero, reflecting purely elastic behavior without energy dissipation. Similarly, as the dynamic Poisson's ratio approaches zero, the material exhibits no lateral deformation, and the Poisson's loss factor approaches zero, indicating no phase lag.

Equation (7) was developed<sup>[82]</sup> to illustrate how this loss factor ratio varies over positive dynamic Poisson's ratios. **Figure 3** extends this concept to auxetic isotropic viscoelastic materials. At a dynamic Poisson's ratio of  $-1$ , the loss factor ratio returns to zero due to the unique deformation behavior of auxetic materials, where lateral and longitudinal strains mirror the applied load. This results in no phase lag and, consequently, no energy dissipation through transverse deformation, reflecting the theoretical limits of energy storage without loss.

For Equation (7) to hold true, the following five key assumptions must be met:<sup>[82]</sup> 1) the solid material is homogeneous and isotropic, 2) the dynamic behavior is linear, 3) the dynamic Poisson's ratio is positive, 4) the shear damping is low, namely,  $\eta_G < 0.3$ , and 5) the ratio of the bulk loss factor to the shear loss factor obeys a power law of the dynamic Poisson's ratio.

Assumptions (1) and (2) hold. Assumption (3) is the focus of our investigation in this article, where we are testing its applicability beyond its initial constraints. Assumption

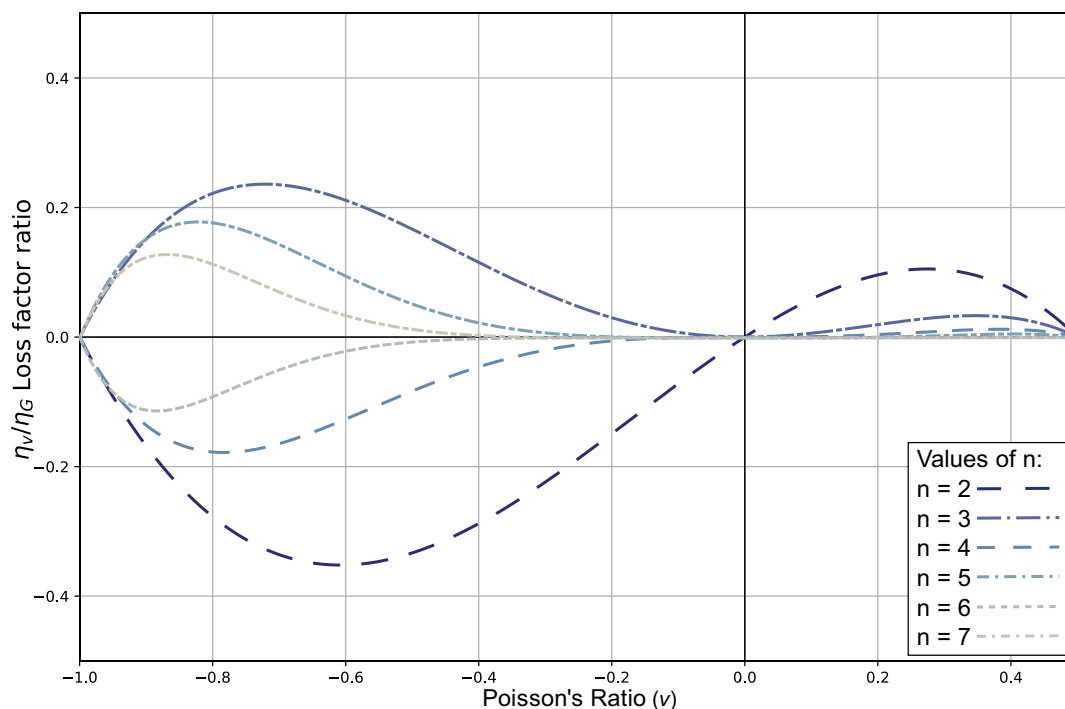


**Figure 3.** Poisson to shear loss factor ratio as a function of dynamic Poisson's ratio ( $-1.0 < \nu_d < 0.5$ ) (for values of  $n=2, 3, 4, 5, 6$ , and  $7$ ) for Equation (7).

(4) remains unverified due to limited data on shear loss factor thresholds in auxetic isotropic viscoelastic materials. However, assumption (5), regarding the ratio of the bulk loss factor to the shear loss factor obeying a power law of the dynamic Poisson's ratio, needs further attention and will be discussed in detail in Section 2.

The Poisson to shear loss factor ratio, as illustrated in Figure 3, can exhibit both negative and positive values, reflecting the complex energy dissipation mechanisms in viscoelastic materials.<sup>[89]</sup> Physically, a negative ratio does not imply that the system gains energy but indicates an imbalance in how energy is dissipated through different deformation modes. Negative values occur when  $n$  is even, due to the  $\nu_d^{n-1}$  component, which results in a negative contribution when the dynamic Poisson's ratio is negative. When  $n$  is even, energy dissipation through transverse deformation is less effective, indicating that auxetic behavior has limited influence on shear loss compared to longitudinal strain. This suggests that auxetic effects, while beneficial for certain bulk properties, may not enhance shear damping in these specific cases.

While the shear loss factor remains finite and positive, it generally dominates the Poisson loss factor ( $\eta_\nu/\eta_G < 0.5$  for Figure 3), which reflects dissipation related to lateral strain induced by axial strain. A negative dynamic Poisson's ratio results in unconventional dissipation behavior, where the Poisson loss factor appears negative due to atypical phase characteristics. Figure 3 shows that the Poisson's loss factor has a greater impact on the loss factor ratio in the auxetic range than in the positive Poisson's ratio range, returning to zero at  $\nu_d$  of  $-1$ ,  $0$ , and  $0.5$  for all values of  $n$ .

## 2.2. Bound Limits for $\eta_K/\eta_G$

Previous works<sup>[87]</sup> established theoretical upper and lower bounds for the loss factor ratio,  $\eta_K/\eta_G$ , in isotropic viscoelastic materials with positive dynamic Poisson's ratio. The upper bound was found at  $\nu_d = 0$ , where the bulk-to-shear loss factor ratio must be  $\leq 1$ , while the lower bound is reproduced in Equation (8). The reader is referred to ref. [87] for further details on their derivation.

$$\frac{\eta_K}{\eta_G} > \frac{1 - 2\nu_d}{1 + \nu_d} \quad (8)$$

In what follows, we will use a similar approach to derive the bounds of  $\eta_K/\eta_G$  for negative Poisson's ratios. Notably, the lower bound of this ratio is  $\eta_K/\eta_G > 1$  when bulk deformation dominates energy dissipation. In such a case, the material exhibits a low bulk modulus but a nonzero shear modulus, as seen in auxetic materials (Figure 2a,b).

As for the upper bound, we consider the complex form of the first Lamé's constant,<sup>[71,85,89]</sup>  $\lambda$ , where Equation (5) can be recast as<sup>[87]</sup>

$$\bar{\lambda}(i\omega) = \lambda_d(\omega)(1 + i\eta_\lambda(\omega)) \quad (9)$$

Equation (9) can be expressed as an isotropic viscoelastic material under dynamic conditions, considering the relation between the complex bulk and complex shear moduli as derived by Tschoegl:<sup>[85]</sup>

$$\bar{K}(i\omega) = \frac{2}{3}\bar{G}(i\omega) \frac{1 + \bar{\nu}(i\omega)}{1 - 2\bar{\nu}(i\omega)} \quad (10)$$

It follows that at  $\nu_d = 0 = \bar{\nu}(i\omega)$ , Equation (9) and (10) can be written as

$$\bar{\lambda}(i\omega) = \bar{K}(i\omega) - \frac{2}{3}\bar{G}(i\omega) = \left(K_d - \frac{2}{3}G_d\right) + i\left(\eta_K K_d - \frac{2}{3}\eta_G G_d\right) \quad (11)$$

Using Equation (3) and (4), Equation (11) can be rewritten using the imaginary parts only:<sup>[78]</sup>

$$i(\eta_\lambda \lambda_d) = i\left(\eta_K K_d - \frac{2}{3}\eta_G G_d\right) \quad (12)$$

Using Equation (12), the Lamé's loss factor ( $\eta_\lambda$ ) can be expressed as a function of the bulk and shear loss factors,  $\eta_K$  and  $\eta_G$ , along with their corresponding dynamic storage moduli,  $K_d$  and  $G_d$ . Theocaris<sup>[89]</sup> suggests that for viscoelastic materials, the shear modulus is greater than the bulk modulus ( $\bar{G} > \bar{K}$ ), implying that both the real and imaginary parts of the shear modulus exceed those of the bulk modulus. This relationship leads to the conditions that the dynamic storage and loss moduli:<sup>[89]</sup>

$$G_d > K_d \quad (13)$$

$$\eta_G G_d > \eta_K K_d \quad (14)$$

Which, in turn, implies that the ratio  $K_d/G_d$  is less than 1. Consequently, this directly supports the inequality in Equation (15), as the left-hand side,  $\frac{\eta_K K_d}{\eta_G G_d}$ , becomes smaller due to the  $K_d/G_d$  term. Given that the ratio of loss factors  $\eta_K/\eta_G$  depends on the material, the inequality will hold if the product of these terms remains less than 2/3 which is supported by Theocaris' observation of the relative magnitudes of the moduli.<sup>[47]</sup>

$$\frac{\eta_K K_d}{\eta_G G_d} < \frac{2}{3} \quad (15)$$

Combining Equation (15) with Equation (6), we obtain the upper bound as a function of dynamic Poisson's ratio when  $\nu_d < 0$ :

$$\frac{\eta_K}{\eta_G} < \frac{1 - 2\nu_d}{1 + \nu_d} \quad (16)$$

Equation (16) now represents the upper bound for dynamic Poisson's ratio from 0 to  $-1.0$ . These bounds are detailed in Figure 4a,b and 5 as dashed red lines.

### 2.3. Bulk-to-Shear Loss Factor Ratio

The ratio of the bulk to the shear loss factor ratio,  $\eta_K/\eta_G$ , can be expressed as follows for isotropic, positive Poisson's ratio viscoelastic solids:<sup>[82]</sup>

$$\frac{\eta_K}{\eta_G} = 1 - (2\nu_d)^n \quad (17)$$

where  $n > 1$ , within the bounds discussed in Section 2.3. To determine whether Equation (17) remains valid for negative dynamic Poisson's ratios, we must revisit and modify the assumptions underlying its derivation.

When extending this analysis to auxetic materials, we assume that the viscoelastic mechanisms influencing loss factors remain consistent, even as the Poisson's ratio approaches  $-1.0$ . For Equation (17) to remain valid, the viscoelastic behavior should not drastically alter due to auxetic characteristics. Typically, as the Poisson's ratio decreases (i.e.,  $\nu_d \rightarrow 0$ ), and we observe that  $\frac{\eta_K K_d}{\eta_G G_d} < 2/3$ , it indicates that the dynamic shear modulus dominates the dynamic bulk modulus, as illustrated in Figure 2b ( $K_d/G_d < 1$ ). If auxetic materials conform to these conditions, Equation (17) remains applicable.

Next, we consider the validity of Equation (17) in the negative dynamic Poisson's ratio range, specifically as  $\nu_d$  approaches 0 or  $-0.5$ . Between these limits, we assume the bulk loss factor exceeds the shear loss factor ( $\eta_K/\eta_G > 1$ ). As the dynamic Poisson's ratio nears zero, the Poisson's loss factor also tends to zero, indicating a lack of transverse motion or phase lag. While the expression  $\eta_\nu = \nu_l/\nu_d = 0/0$  is mathematically undefined, we can approximate that the  $\eta_\nu \rightarrow 0$  as  $\nu_d \rightarrow 0$ , as shown in Figure 3. In the case of  $\nu_d = -0.5$ , the material experiences a unique balance between lateral and axial deformations, resulting in enhanced volumetric stability and energy dissipation characteristics. The relationship between the bulk and shear moduli leads to a specific condition where the bulk loss factor becomes exactly twice that of the shear loss factor ( $\eta_K/\eta_G = 2$ ) as shown in Figure 4a, indicating that the material exhibits a significant response in bulk loss compared to shear loss, reflecting its auxetic nature. Therefore, for dynamic Poisson's ratios near  $-0.5$ , the Poisson to shear loss factor ratio can be approximated by the following equation:<sup>[87]</sup>

$$\frac{\eta_\nu}{\eta_G} \approx \left(1 - \frac{\eta_K}{\eta_G}\right) \frac{(1 + \nu_d)(1 - 2\nu_d)}{3\nu_d} \quad (18)$$

assuming  $\eta_K/\eta_G > 1$  for auxetic isotropic viscoelastic materials.

For the case where the dynamic Poisson's ratio approaches  $-0.5$ , Figure 4a shows that  $\eta_K/\eta_G$  is equal to 2 and we can approximate part of Equation (18) as:

$$\left(1 - \frac{\eta_K}{\eta_G}\right) \frac{(1 + \nu_d)}{3\nu_d} \approx \frac{1}{3} \quad (19)$$

This implies that the Poisson's loss factor compared to the shear loss factor can still depend only on the dynamic Poisson's ratio, as approximated by developing Equation (18) and (19) into

$$\frac{\eta_\nu}{\eta_G} \approx \frac{1}{3}(1 - 2\nu_d) \quad (20)$$

For Equation (18), when dynamic Poisson's ratio approaches zero, it can be approximated to

$$\frac{\eta_\nu}{\eta_G} \approx \left(1 - \frac{\eta_K}{\eta_G}\right) \frac{1}{3\nu_d} \quad (21)$$

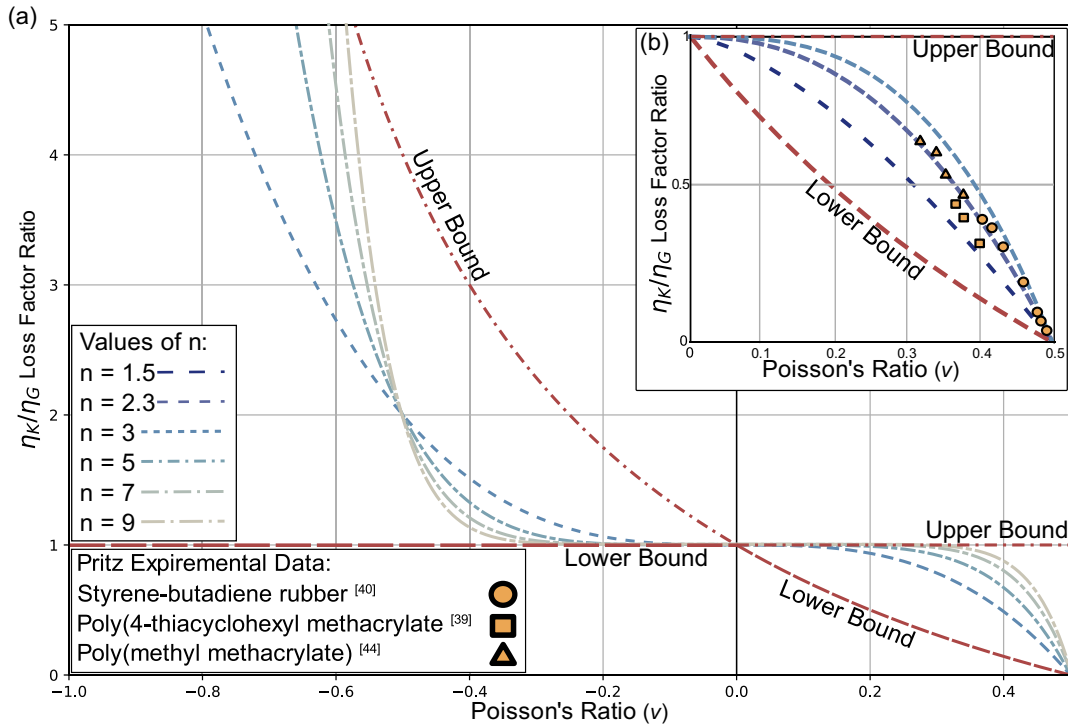


**Figure 4.** Bulk-to-shear loss factor ratio as a function of dynamic Poisson's ratio of Equation (17)<sup>[87]</sup> for a) dynamic Poisson's range ( $-1.0 < \nu_d < 0.5$ ) for values of  $n = 3, 5, 7,$  and  $9$  and b) positive Poisson's ratio relationship ( $0.0 < \nu_d < 0.5$ ) for values of  $n = 1.5, 2.3,$  and  $3.0$  alongside experimental data for SBR,<sup>[81]</sup> PMMA,<sup>[90]</sup> and P4OCHMA.<sup>[80]</sup>

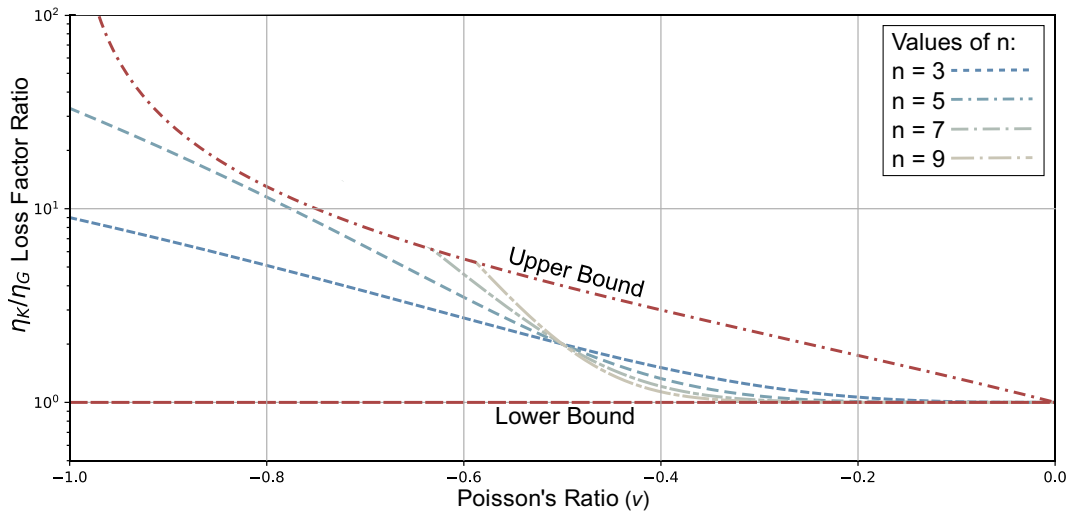


**Figure 5.** Bulk-to-shear loss factor ratio (Log) ( $0.1 < \eta_K/\eta_G < 100$ ) as a function of dynamic Poisson's ratio ( $-1.0 < \nu_d < 0$ ) of Equation (17) showing values of  $n = 3, 5, 7,$  and  $9$  and upper and lower bound limits.

Here, the bulk loss factor converges to the shear loss factor ( $\eta_K \rightarrow \eta_G$ ) as the dynamic Poisson ratio tends to zero ( $\nu_d \rightarrow 0$ ), resulting in the Poisson's loss factor approaching zero. Equation (17) holds true if  $(1 - \eta_K/\eta_G)$  can be expressed as a function of its dynamic Poisson's ratio, such as the development of Equation (21) below:<sup>[41]</sup>

$$1 - \frac{\eta_K}{\eta_G} = a\nu_d^n \quad (22)$$

where  $a > 0$  and  $n > 1$  under the assumption that auxetic isotropic viscoelastic materials maintain the dominance of the

bulk loss factor over the shear loss factor, and then Equation (20) and (22) confirm that Equation (17) remains valid.

The exponent  $n > 1$  reflects an empirical fit to data and can vary between materials and ranges of dynamic Poisson's ratio. While  $n$  can be adjusted to fit experimental data, even for auxetic materials, values of  $n$  must be odd integers under the assumptions outlined in this study. This constraint ensures that this loss factor remains physically meaningful (i.e., nonnegative) over the full range of dynamic Poisson's ratios, particularly below  $\nu_d = -0.5$ . If  $n$  were even, the loss factor would become negative for dynamic Poisson's ratios below this threshold.  $n$  must remain an integer to maintain the validity of Equation (22) when dynamic Poisson's ratio is less than zero, ensuring the model applies consistently across both positive and negative Poisson's ratio ranges (Figure 4a). Experimental data from Pritz's 2007<sup>[82]</sup> study support the variability in  $n$  across different materials such as styrene-butadiene rubber (SBR),<sup>[81]</sup> poly(methyl methacrylate) (PMMA),<sup>[90]</sup> and poly(4-thiacyclohexyl methacrylate) (P4OCHMA),<sup>[80]</sup> suggesting a broader applicability beyond strictly positive Poisson's ratios. Figure 4b illustrates how variations in  $n$  ( $n = 1.5, 2.3, \text{ and } 3.0$ ) affect the bulk-to-shear loss factor ratio, with  $n = 2.3$  offering the best fit to the provided data over a positive dynamic Poisson's ratio. This emphasizes the need to adjust  $n$  to account for specific material behavior, especially in auxetic cases.

In conclusion, it is reasonable to extend the application of Equation (17) to auxetic materials, provided the assumptions about viscoelastic response, the bulk-to-shear loss factor constraints, and the appropriate value of  $n$  are satisfied. However, deviations from these assumptions may require experimental validation or adjustments to the equation.

### 3. Results and Discussion

The relationship between the dynamic shear and bulk moduli across both auxetic and positive dynamic Poisson's ratios is well established (Equation 1 and 2). As Poisson's ratio approaches  $-1$ , the dynamic shear storage modulus increases, indicating heightened stiffness in shear deformation (Figure 2a). In contrast, the dynamic bulk storage modulus decreases, suggesting a reduced capacity for the viscoelastic solid to resist volumetric changes and store elastic energy. This is illustrated by the ratio of dynamic bulk-to-shear storage moduli ( $K_d/G_d$ ) in Figure 2b, derived from Equation (6). The figure shows that below a Poisson's ratio of 0.1, the dynamic shear modulus dominates, while above 0.1, the dynamic bulk modulus becomes more dominant.

This work examines the relationship between dynamic Poisson's ratio and the ratios of both the Poisson to shear loss factors ( $\eta_\nu/\eta_G$ ) and the bulk-to-shear loss factors ( $\eta_K/\eta_G$ ), extending the work of Pritz in the positive dynamic Poisson's ratio range ( $0 < \nu_d < 0.5$ ).<sup>[82,87]</sup> Pritz demonstrated that there was a link over  $0 < \nu_d < 0.5$ , distinct-bound limits and at  $\nu_d = 0.5$  the bulk-to-shear loss factor ratio can be wide ranging compared to those a  $\nu_d \approx 0$  (Figure 2b).

Equation (17), which predicts the bulk-to-shear loss factor ratio, can be extended into the auxetic range for isotropic viscoelastic materials, provided the assumptions in Section 2 are met. Although the bulk-to-shear loss factor ratio for auxetic materials

can vary widely, most results likely lie within the upper and lower bounds discussed in Section 2. The exponent  $n$  is essential for tailoring the equation to different materials, but it may not predict material behavior across the entire dynamic Poisson's ratio range. In the positive Poisson range, power factors of 1.5, 2.3, and 3.0 are shown in Figure 4b, while Figure 4a presents the results for auxetic materials ( $1 < \eta_K/\eta_G < \frac{1-2\nu_d}{1+\nu_d}$ ). Power factors of 3, 5, 7, and 9 are considered for auxetic materials, but Equation (17) is only likely to predict behavior over a narrow range of Poisson's ratios for certain materials. Further experimental work on auxetic viscoelastic solids is needed to validate these findings.

All lines intersect at three key points within the dynamic Poisson's ratio range shown in Figure 4. The intersections at  $\nu_d$  of 0 and 0.5, previously identified for positive Poisson's ratios, represent incompressibility ( $\nu_d = 0.5$ ) and no lateral strain ( $\nu_d = 0$ ). A notable feature is the new intersection at  $\nu_d = -0.5$ , observed for all odd integer values of  $n$ , with a bulk-to-shear loss factor ratio of 2 ( $\eta_K/\eta_G = 2$ ). This indicates that bulk deformation contributes twice as much to energy dissipation as shear deformation at this Poisson's ratio. The relationship between volumetric strain ( $\varepsilon_V$ ) and axial strain ( $\varepsilon_{\text{axial}}$ ) is given by

$$\varepsilon_V = \varepsilon_{\text{axial}}(1 - 2\nu_d) \quad (23)$$

At  $\nu_d = 0.5$ ,  $\varepsilon_V$  becomes zero, confirming incompressibility, while at  $\nu_d = -0.5$ ,  $\varepsilon_V = 2$ , showing an apparent volume increase under uniaxial deformation despite the lateral and transverse strains counteracting the axial deformation.

The wide range of bulk-to-shear loss factor values as the dynamic Poisson's ratio approaches  $-1.0$  (shown in Figure 5) depends on the energy dissipation mechanisms, which are complex in auxetic materials. These materials depend on their microstructure, influencing how bulk and shear deformations occur. The loss factors, which are frequency-dependent, show that at certain frequencies, bulk viscosity dominates energy dissipation in isotropic viscoelastic materials, especially as Poisson's ratio becomes negative. Equation (17) can predict behavior for a limited range of viscoelastic materials when an appropriate power factor  $n$  is chosen. It does not hold true across the entire dynamic Poisson's ratio range, particularly for larger values of  $n$  (exceeding  $n = 7$ ) as they may extend outside the suggested bound limits.

Auxetic (by microstructure) metamaterials can exhibit changeable density for certain viscoelastic materials (such as polymers, foams, or composites); the bulk modulus could be designed or tuned to have higher internal friction or more significant energy loss mechanisms than the shear modulus under dynamic conditions. The density of these foams is not constant but varies with the amount of applied stress or strain. Under rapid loading, the internal microstructure of the foam might exhibit enhanced reentrant behavior or chiral cell deformation, which could result in different damping characteristics than under static or slow loading conditions. This ability to be able to tailor their density would play a crucial role in determining their bulk modulus at lower Poisson's ratios. The density of these foams is not constant but varies with the amount of applied stress or strain. This variability in density is a key property, as it directly impacts

the mechanical characteristics of the material, particularly the bulk modulus. The bulk modulus, which defines a material's resistance to uniform compression, will change as the density changes, making auxetic foams highly adaptable to different loading conditions. The unique way the internal structure responds to localized deformation especially around dynamic Poisson's ratio around  $-1$  and the bulk-to-shear loss factor ratio leads to unique damping characteristics. The ability to tailor the density and microstructure of auxetic foams opens new possibilities for designing materials with specific mechanical properties. For instance, in applications like protective gear, vibration isolation, or acoustic dampening, where a high bulk-to-shear loss factor ratio is desirable, auxetic foams could be designed to perform better than traditional materials. Although this work is theoretical, auxetic materials such as reentrant polyurethane foams,<sup>[10,63,91]</sup> though not strictly isotropic, are often considered quasi-isotropic in their auxetic behavior and are representative examples of auxetic materials. These foams exhibit properties such as a high bulk-to-shear loss factor ratio,<sup>[92]</sup> making them ideal for applications like protective gear, vibration isolation, or acoustic dampening.

#### 4. Conclusion

In this article, we investigated the dynamic behavior, limited to isotropic auxetic viscoelastic solids, focusing on the relationships between dynamic bulk and shear storage moduli, Poisson's ratio, and energy dissipation characteristics. Building on Pritz's work from 2007<sup>[82]</sup> and 2009,<sup>[87]</sup> we confirmed that the bulk-to-shear loss factor ratio can be effectively predicted for auxetic materials using modified assumptions of Equation (17). Our findings show that the bulk loss factor dominates over the shear loss factor when the exponent  $n$  in the equation is a positive odd integer, and we established the bound limits for auxetic materials.

We extended existing theories by demonstrating that the relationships linking the bulk and shear moduli to Poisson's ratio remain valid in the negative Poisson's ratio range. Specifically, we analyzed how these relationships influence energy dissipation through Poisson to shear loss factor ratios and bulk-to-shear loss factor ratios, including their bound limits. The analysis within the auxetic range, limited to isotropic viscoelastic materials, is valid as long as the following five key assumptions were satisfied: the solid material is homogeneous and isotropic, its dynamic behavior is linear, the dynamic Poisson's ratio is positive, the shear damping is low ( $\eta_G < 0.3$ ), and the ratio of the bulk loss factor to the shear loss factor follows a power law relationship with the dynamic Poisson's ratio, as described in Equation (7).

Future research should extend Pritz and Tschoegl's work to accommodate orthotropic or anisotropic auxetic viscoelastic materials. Experimental data across a wider range of materials are needed to validate and refine these predictive models. Insights would benefit applications in defense, sports, and devices experiencing dynamic nonlinear vibrations, where enhanced damping and energy absorption properties are crucial.

#### Acknowledgements

This research was supported by the UK Engineering and Physical Sciences Research Council (EPSRC).

#### Conflict of Interest

The authors declare no conflict of interest.

#### Data Availability Statement

Data sharing is not applicable to this article as no new data were created or analyzed in this study.

#### Keywords

auxetic, bulk, loss factors, shear, viscoelasticity

Received: September 26, 2024

Revised: February 14, 2025

Published online:

- [1] K. E. Evans, M. A. Nkansah, I. J. Hutchinson, S. C. Rogers, *Nature* **1991**, 353, 124.
- [2] S. Poisson, Mémoires de l'Académie Royale Des Sciences de l'Institut de France **1829**, 9, 273.
- [3] K. W. Wojciechowski, *Phys. Lett. A* **1989**, 137, 60.
- [4] K. W. Wojciechowski, *J. Phys. A: Math. Gen.* **2003**, 36, 11765.
- [5] R. H. Baughman, J. M. Shacklette, A. A. Zakhidov, S. Stafströ, *Nature* **1998**, 392, 362.
- [6] K. E. Evans, A. Alderson, *Adv. Mater.* **2000**, 12, 617.
- [7] W. Wu, W. Hu, G. Qian, H. Liao, X. Xu, F. Berto, *Mater Des.* **2019**, 180, 107950.
- [8] Q. Yang, Z. Li, H. Hao, W. Chen, *Eng. Struct.* **2023**, 281, 115751.
- [9] E. Zhang, Y. Chen, E. A. Nasr, *Mech. Adv. Mater. Struct.* **2023**, 31, 9387.
- [10] R. Lakes, *Science* **1987**, 235, 1038.
- [11] F. Scarpa, L. G. Ciffo, J. R. Yates, *Smart Mater. Struct.* **2004**, 13, 49.
- [12] Y. Ma, F. Scarpa, D. Zhang, B. Zhu, L. Chen, J. Hong, *Smart Mater. Struct.* **2013**, 22, 084012.
- [13] S. K. Bhullar, *e-Polymers* **2015**, 15, 205.
- [14] T. C. Lim, in *Mechanics of Metamaterials With Negative Parameters*, Springer, Singapore **2020**.
- [15] T. C. Lim, *Phys. Status Solidi RRL* **2017**, 11, 1600440.
- [16] M. Bilski, K. W. Wojciechowski, T. Stręk, P. Kędziora, J. N. Grima-Cornish, M. R. Dudek, *Materials* **2021**, 14, 7837.
- [17] J. W. Narojczyk, M. Bilski, J. N. Grima, P. Kędziora, D. Morozow, M. Rucki, K. W. Wojciechowski, *Materials* **2022**, 15, 1134.
- [18] K. V. Tretyakov, K. W. Wojciechowski, *Phys. Status Solidi B* **2005**, 242, 730.
- [19] R. Lakes, *Nature* **2001**, 410, 565.
- [20] G. Hartwig, in *Nonmetallic Materials and Composites at Low Temperatures*, Springer US, Boston **1979**.
- [21] J. Grima, P. S. Farrugia, R. Gatt, V. Zammit, *J. Phys. Soc. Jpn.* **2007**, 76, 025001.
- [22] J. Grima, R. Gatt, V. Zammit, R. Cauchi, in *Industrial Applications of Molecular Simulations, Vol. 1*, CRC Press, Boca Raton **2012**.
- [23] Z. F. Sang, Z. Y. Li, *Phys. Lett.* **2005**, 334, 422.
- [24] R. Lakes, K. W. Wojciechowski, *Phys. Status Solidi B* **2008**, 245, 545.

- [25] T. Strek, B. Maruszewski, J. W. Narojczyk, K. W. Wojciechowski, *J. Non-Cryst. Solids* **2008**, 354, 4475.
- [26] A. A. Poźniak, K. W. Wojciechowski, J. N. Grima, L. Mizzi, *Composites, Part B* **2016**, 94, 379.
- [27] J. N. Grima, R. Caruana-Gauci, D. Attard, R. Gatt, *Proc. R. Soc. A: Math. Phys. Eng. Sci.* **2012**, 468, 3121.
- [28] R. Ruppin, *Solid State Commun.* **2000**, 116, 411.
- [29] A. Mrozek, T. Strek, *Materials* **2022**, 15, 8712.
- [30] T. Strek, J. Michalski, H. Jopek, *Phys. Status Solidi B* **2019**, 256, 1800423.
- [31] T. Strek, *Vib. Phys. Syst.* **2018**, 29, 2018003.
- [32] Y. Zhu, S. Jiang, Q. Zhang, J. Li, C. Yu, C. Zhang, *Int. J. Mech. Sci.* **2022**, 236, 107750.
- [33] S. Shukla, B. K. Behera, *Compos. Struct.* **2022**, 290, 115530.
- [34] G. Stokes, *Trans. Cambridge Philos. Soc.* **1851**, 3, 1880.
- [35] L. J. Gibson, M. F. Ashby, G. S. Schajer, C. I. Robertson, *Proc. R. Soc. Lond. A* **1982**, 382, 25.
- [36] A. G. Kolpakov, *J. Appl. Math. Mech.* **1985**, 49, 739.
- [37] R. F. Almgren, *J. Elasticity* **1985**, 15, 427.
- [38] K. W. Wojciechowski, *Mol. Phys.* **1987**, 61, 1247.
- [39] A. Hosseinkhani, D. Younesian, M. Ranjbar, F. Scarpa, *Appl. Acoust.* **2021**, 177, 107930.
- [40] B. Howell, P. Prendergast, L. Hansen, *Appl. Acoust.* **1994**, 43, 141.
- [41] A. A. Saddek, T. K. Lin, W. K. Chang, C. H. Chen, K. C. Chang, *Materials* **2023**, 16, 5499.
- [42] N. Shi, H. Liu, L. Wang, J. Ji, Z. Li, S. Guo, J. Wang, *Europhys. Lett.* **2023**, 144, 20001.
- [43] S. Faroughi, M. Shaat, *Eur. J. Mech.* **2017**, 70, 8.
- [44] K. Billon, I. Zampetakis, F. Scarpa, M. Ouisse, E. Sadoulet-Reboul, M. Collet, A. Perriman, A. Hetherington, *Compos. Struct.* **2017**, 160, 1042.
- [45] A. T. Mathis, N. N. Balaji, R. J. Kuether, A. R. Brink, M. R. W. Brake, D. D. Quinn, *Appl. Mech. Rev.* **2020**, 72, 040802.
- [46] Q. Zhang, X. Yu, F. Scarpa, D. Barton, Y. Zhu, Z. Q. Lang, D. Zhang, *Mech. Syst. Signal Process.* **2022**, 179, 109375.
- [47] V. A. Skripnyak, M. O. Chirkov, V. V. Skripnyak, *J. Sib. Fed. Univ.* **2024**, 2024, 91.
- [48] J. Michalski, T. Strek, in *Advances in Manufacturing III*, Springer, Cham **2022**.
- [49] N. Novak, M. Borovinšek, O. Al-Ketan, Z. Ren, M. Vesenjak, *Compos. Struct.* **2022**, 300, 116174.
- [50] Y.-M. Yi, S.-H. Park, S.-K. Youn, *Int. J. Solids Struct.* **2000**, 37, 4791.
- [51] R. P. Bohara, S. Linforth, T. Nguyen, A. Ghazlan, T. Ngo, *Eng. Struct.* **2023**, 276, 115377.
- [52] N. Novak, M. Nowak, M. Vesenjak, Z. Ren, *Phys. Status Solidi B* **2022**, 259, 2200409.
- [53] A. Airoidi, N. Novak, F. Sgobba, A. Gilardelli, M. Borovinšek, *Mater. Sci. Eng., A* **2020**, 788, 139500.
- [54] B. Howell, L. Hansen, P. Prendergast, DTRC-SME-91/01, David Taylor Research Center, Annapolis, MD **1991**. <https://apps.dtic.mil/sti/tr/pdf/ADA235695.pdf>.
- [55] M. Sanami, N. Ravirala, K. Alderson, A. Alderson, *Proc. Eng.* **2014**, 72, 453.
- [56] S. Shukla, B. K. Behera, *J. Text. Inst.* **2023**, 114, 1078.
- [57] A. V. Mazaev, O. Ajenez, M. V. Shitikova, *IOP Conf. Ser. Mater. Sci. Eng.* **2020**, 747, 012008.
- [58] X. Zhou, K. Parida, J. Chen, J. Xiong, Z. Zhou, F. Jiang, Y. Xin, S. Magdassi, P. S. Lee, *Adv. Energy Mater.* **2023**, 13, 2301159.
- [59] T. Fey, F. Eichhorn, G. Han, K. Ebert, M. Wegener, A. Roosen, K. I. Kakimoto, P. Greil, *Smart Mater. Struct.* **2016**, 25, 015017.
- [60] A. Gaur, S. Meena, N. Meena, N. Saurabh, S. Patel, *Ferroelectrics* **2024**, 618, 274.
- [61] M. Ravanbod, S. Ebrahimi-Nejad, *Mech. Adv. Mater. Struct.* **2023**, 31, 9857.
- [62] J. W. Narojczyk, K. V. Tretiakov, J. Smardzewski, K. W. Wojciechowski, *Phys. Rev E* **2023**, 108, 045003.
- [63] F. Scarpa, C. Remilat, F. P. Landi, G. Tomlinson, in *Proc. SPIE Smart Struct. Mater. 2000: Damping and Isolation*, International Society for Optics and Photonics, Orlando, FL; Bellingham, WA **2000**, 3989, 336.
- [64] N. Mortazavi, S. Ziaei-Rad, *Mech. Adv. Mater. Struct.* **2024**, 0, 1.
- [65] Q. He, J. Zhu, L. Li, Y. Guo, D. Yan, *J. Mech. Mater. Struct.* **2024**, 19, 435.
- [66] R. Telukunta, in *Constrained Layer Damping of Honeycomb Composite*, Clemson University, USA **2011**.
- [67] A. Matuszewska, T. Strek, *Vib. Phys. Syst.* **2018**, 29, 2018031.
- [68] R. Galea Mifsud, G. A. Muscat, J. N. Grima-Cornish, K. K. Dudek, M. A. Cardona, D. Attard, P. S. Farrugia, R. Gatt, K. E. Evans, J. N. Grima, *Materials* **2024**, 17, 1506.
- [69] T. Strek, A. Matuszewska, H. Jopek, *Phys. Status Solidi B* **2017**, 254, 1700103.
- [70] T. Strek, H. Jopek, E. Idczak, K. W. Wojciechowski, *Materials* **2017**, 10, 1386.
- [71] N. W. Tschoegl, W. G. Knauss, I. Emri, *Mech. Time-Depend. Mater.* **2002**, 6, 3.
- [72] H. A. Waterman, *Rheol. Acta* **1977**, 16, 31.
- [73] P. Dewangan, *Master Thesis*, National Institute of Technology, Rourkela **2009**.
- [74] Y. V. K. Sadasiva Rao, B. C. Nakra, *J. Sound Vib.* **1974**, 34, 309.
- [75] C. Raposo, *Mathematica Moravica* **2021**, 25, 53.
- [76] P. J. Shorter, *J. Acoust. Soc. Am.* **2004**, 115, 1917.
- [77] K. R. Karim, G. D. Chen, *Mech. Syst. Signal Process.* **2012**, 27, 419.
- [78] M. H. Sadd, in *Elasticity-Theory, Applications and Numerics*, Elsevier, MA, USA **2009**.
- [79] F. M. Guillot, D. H. Trivett, *J. Sound Vib.* **2011**, 330, 3334.
- [80] J. Heijboer, L. C. E. Struik, H. A. Waterman, M. P. Van Duijkeren, *J. Macromol. Sci. B* **1971**, 5, 375.
- [81] Y. Wada, R. Ito, H. Ochiai, *J. Phys. Soc. Jpn.* **1962**, 17, 213.
- [82] T. Pritz, *J. Sound Vib.* **2007**, 306, 790.
- [83] A. Wineman, *Math. Mech. Solids* **2009**, 14, 300.
- [84] R. S. Lakes, A. Wineman, *J. Elasticity* **2006**, 85, 45.
- [85] N. W. Tschoegl, in *The Phenomenological Theory of Linear Viscoelastic Behavior*, Springer, Berlin; Heidelberg **1989**.
- [86] X. Q. Zhou, D. Y. Yu, X. Y. Shao, S. Q. Zhang, S. Wang, *Compos. Struct.* **2016**, 136, 460.
- [87] T. Pritz, *J. Sound Vib.* **2009**, 324, 514.
- [88] T. Meier, R. Li, S. Mavrikos, B. Blankenship, Z. Vangelatos, M. E. Yildizdag, C. P. Grigoropoulos, *NPJ Comput. Mater.* **2024**, 10, 3.
- [89] P. S. Theocaris, *Kolloid Z. Z. Polym.* **1969**, 235, 1182.
- [90] A. F. Yee, M. T. Takemori, *J. Polym. Sci.: Polym. Phys. Ed.* **1982**, 20, 205.
- [91] S. Shilko, D. Konyok, *Comput. Methods Sci. Technol.* **2004**, 10, 197.
- [92] E. O. Martz, T. Lee, R. S. Lakes, V. K. Goel, *Cell. Polym.* **1996**, 15, 229.